Theor Chem Acc (2011) 130:701–709
DOI 10.1007/s00214-011-0964-2

REGULAR ARTICLE

Finite-field evaluation of static (hyper)polarizabilities based on the linear-scaling divide-and-conquer method

Tsuguki Touma · Masato Kobayashi · Hiromi Nakai

Received: 27 December 2010 / Accepted: 16 May 2011 / Published online: 4 June 2011

Abstract This article describes the finite-field (FF) approach for calculating static (hyper)polarizabilities based on the divide-and-conquer (DC) method. The method is assessed by the Hartree–Fock (HF) and post-HF calculations of π-conjugated model systems: a terminal donor or acceptor substituent on polyene chains. The DC–FF approach enables the evaluation of molecular polarizabilities with highly accurate coupled-cluster theory. Numerical assessments demonstrate that the (hyper)polarizabilities calculated by the present DC–FF method agree with the conventional FF results to within a few percent by employing an appropriate buffer size.

Keywords Divide-and-conquer · Finite-field method · Hyperpolarizability · Linear-scaling · Nonlinear optics · Correlation theory

Dedicated to Professor Akira Imamura on the occasion of his 77th birthday and published as part of the Imamura Festschrift Issue.

T. Touma · M. Kobayashi · H. Nakai (✉)
Department of Chemistry and Biochemistry,
School of Advanced Science and Engineering,
Waseda University, Tokyo 169-8555, Japan
e-mail: nakai@waseda.jp

M. Kobayashi · H. Nakai
Department of Theoretical and Computational Molecular Science, Institute for Molecular Science,
Okazaki 444-8585, Japan

H. Nakai
Research Institute for Science and Engineering,
Waseda University, Tokyo 169-8555, Japan

H. Nakai
CREST, Japan Science and Technology Agency,
Tokyo 102-0075, Japan

1 Introduction

In recent years, nonlinear optical materials have received a lot of attention due to their potential utilization in electro-optical devices [1–4]. Organic π-conjugated systems, such as a polyene chain, are of particular interest because their properties can be easily changed by chemical modification. Therefore, various theoretical studies on the design of nonlinear optical molecules, polymers, and other materials with desired properties have been performed so far. As part of these studies, there have been attempts to evaluate the nonlinear optical properties by ab initio calculations. However, ab initio quantum chemical treatment of the nonlinear optical materials is difficult in the standard fashion because of its high computational scaling with respect to the system size. To enable large-scale ab initio calculations, several groups have proposed the linear-scaling electronic structure methods.

Development of linear-scaling self-consistent field (SCF) molecular orbital (MO) method started from the pioneering work by Imamura et al. [5] in 1991. Their elongation method was firstly proposed as the theoretical polymerization scheme for treating 1-D periodic and aperiodic polymers at Hartree–Fock (HF) or semi-empirical MO level of theory. Since their invention, the applicability of the elongation method has been extended; e.g., to Kohn–Sham density functional theory (DFT) [6], to post-HF correlation calculation as typified by the second-order Møller–Plesset perturbation (MP2) theory [7], and to the orbital-restricted open-shell treatment [8]. In addition, its efficiency has been also improved in terms of localization schemes [9], a cut-off technique [10], and the quantum fast multipole method [11]. More recently, Aoki and Gu [12] proposed a generalized elongation method that can treat 2-D and 3-D systems by virtue of the defrosting scheme.

Thus, now the elongation method is regarded as a powerful tool that can treat large (super)molecular systems with reasonable accuracy.

Coincidentally, in 1991, Yang [13] proposed another linear-scaling SCF scheme based on the density partitioning in the framework of DFT. His divide-and-conquer (DC) approach was evolved in the one-electron density matrix formalism with atomic basis functions [14] and then became applicable to HF or semi-empirical MO calculations as well as hybrid DFT functionals. However, to the best knowledge of the authors, the first practical implementation and assessment of the DC method including HF exchange interactions (i.e., DC–HF and DC hybrid DFT) were proceeded by the authors' group [15, 16]. We have further proposed the DC-based post-HF correlation schemes [17–21], open-shell treatment with unrestricted orbitals [22], energy gradient method [23], and static and dynamic polarizability calculation method with the time-dependent coupled-perturbed (TDCP) equations [24]. Our extensions of DC method and implementation to the GAMESS package [25] are summarized in recent reviews [26, 27].

The linear-scaling methods, especially the elongation method, have been also utilized to obtain the nonlinear optical properties of large systems by the finite-field (FF) method [28–34]. Although the reported elongation-FF (hyper)polarizabilities spectacularly agree with the actual FF results, these calculations were performed with the semi-empirical or HF theories. In the fragment molecular orbital (FMO) method [35, 36], which is being popular in calculations of large biomolecules and molecular clusters, Mochizuki and coworkers proposed a scheme to evaluate static and dynamic polarizabilities by means of the TDCP equations [37, 38], as the authors proposed in the framework of the DC method [24]. However, these methods have not been applied to the hyperpolarizability calculations so far. Furthermore, there have been no reports that apply the DC method to the FF evaluation of the nonlinear optical properties.

In this paper, we assessed the FF method based on the linear-scaling DC–HF and correlation theories for calculating the static (hyper)polarizabilities. The organization of this article is as follows. Section 2 presents theoretical aspects of the present study, namely, the FF evaluation of the static (hyper)polarizabilities and the DC–HF and correlation methods. The present DC–FF method is numerically assessed in calculations of the polyene chains and their derivatives in Sect. 3. Finally, we give concluding remarks in Sect. 4.

2 Theoretical aspects

At first, we briefly summarize the FF evaluation of molecular (hyper)polarizabilities. The total energy $W(E)$ in the presence of the external electric field E is expanded as

$$W(E) = W(0) - \sum_{\eta_1} \left.\frac{\partial W(E)}{\partial E_{\eta_1}}\right|_{E=0} E_{\eta_1} - \frac{1}{2}\sum_{\eta_1,\eta_2} \left.\frac{\partial^2 W(E)}{\partial E_{\eta_1}\partial E_{\eta_2}}\right|_{E=0} E_{\eta_1}E_{\eta_2} - \frac{1}{6}\sum_{\eta_1,\eta_2,\eta_3} \left.\frac{\partial^3 W(E)}{\partial E_{\eta_1}\partial E_{\eta_2}\partial E_{\eta_3}}\right|_{E=0} E_{\eta_1}E_{\eta_2}E_{\eta_3} - \frac{1}{24}\sum_{\eta_1,\eta_2,\eta_3,\eta_4} \left.\frac{\partial^4 W(E)}{\partial E_{\eta_1}\partial E_{\eta_2}\partial E_{\eta_3}\partial E_{\eta_4}}\right|_{E=0} E_{\eta_1}E_{\eta_2}E_{\eta_3}E_{\eta_4} - \ldots, \tag{1}$$

where $W(0)$ is the field-free total energy and η_i represents Cartesian axis ($\eta_i = x$, y, or z). Thus, the molecular polarizability (α), first hyperpolarizability (β), and second hyperpolarizability (γ) tensors can be obtained as follows:

$$\alpha_{\eta_1\eta_2} = \left.\frac{\partial^2 W(E)}{\partial E_{\eta_1}\partial E_{\eta_2}}\right|_{E=0}, \tag{2}$$

$$\beta_{\eta_1\eta_2\eta_3} = \left.\frac{\partial^3 W(E)}{\partial E_{\eta_1}\partial E_{\eta_2}\partial E_{\eta_3}}\right|_{E=0}, \tag{3}$$

$$\gamma_{\eta_1\eta_2\eta_3\eta_4} = \left.\frac{\partial^4 W(E)}{\partial E_{\eta_1}\partial E_{\eta_2}\partial E_{\eta_3}\partial E_{\eta_4}}\right|_{E=0}. \tag{4}$$

For quasi 1-D systems, such as those considered in this paper, the diagonal elements in the longitudinal direction (z) are the most important. Numerical expressions for these elements with energies at five electric fields are given in [30]:

$$\alpha_{zz} = \frac{W(+2E_z) - 16W(+E_z) + 30W(0) - 16W(-E_z) + W(-2E_z)}{12E_z^2}, \tag{5}$$

$$\beta_{zzz} = \frac{-W(+2E_z) + 2W(+E_z) - 2W(-E_z) + W(-2E_z)}{2E_z^3}, \tag{6}$$

$$\gamma_{zzzz} = \frac{-W(+2E_z) + 4W(+E_z) - 6W(0) + 4W(-E_z) - W(-2E_z)}{E_z^4}. \tag{7}$$

In this paper, the energies obtained from the DC calculations are applied to $W(E)$. In the DC–HF theory, the closed-shell density matrix of the entire system under the external field E is constructed from subsystem contributions as

$$\mathbf{D}(E) = \sum_s \mathbf{D}^s(E). \tag{8}$$

$\mathbf{D}^s(E)$ represents the field-dependent local density matrix for the subsystem s, which is expanded by subsystem bases consisting of two types of atomic orbitals (AOs): one is central AOs [$\boldsymbol{S}(s)$] that belong to the subsystem s itself, called the "central region", and the other is environmental AOs [$\boldsymbol{B}(s)$] that belong to the neighboring region of the subsystem s, called the "buffer region". The union of the central and buffer regions is called the "localization region". $\mathbf{D}^s(E)$ is obtained by using the uniquely defined Fermi level $\varepsilon_{\mathrm{F}}(E)$ and Fermi function $f_{\beta_{\mathrm{temp}}}(x) = [1+\exp(-\beta_{\mathrm{temp}}x)]^{-1}$ with the inverse temperature parameter β_{temp} as

$$D^s_{\mu\nu}(E) = 2p^s_{\mu\nu}\sum_q f_{\beta_{\mathrm{temp}}}[\varepsilon_{\mathrm{F}}(E) - \varepsilon^s_q(E)]C^s_{\mu q}(E)C^{s*}_{\nu q}(E), \tag{9}$$

where q runs over all subsystem MOs and $\mathbf{p}^s$ is the partition matrix defined as

$$p^s_{\mu\nu} = \begin{cases} 1 & \mu \in \boldsymbol{S}(s) \text{ and } \nu \in \boldsymbol{S}(s) \\ 1/2 & [\mu \in \boldsymbol{S}(s) \text{ and } \nu \in \boldsymbol{B}(s)] \text{ or } [\mu \in \boldsymbol{B}(s) \text{ and } \nu \in \boldsymbol{S}(s)] \\ 0 & \text{otherwise.} \end{cases} \tag{10}$$

$\mathbf{C}^s(E)$ and $\varepsilon^s(E)$ are the field-dependent orbital coefficients and energies for the subsystem s, which are the solutions of the following local eigenvalue problem:

$$\mathbf{F}^s(E)\mathbf{C}^s(E) = \mathbf{S}^s\mathbf{C}^s(E)\varepsilon^s(E). \tag{11}$$

Here, $\mathbf{S}^s$ is the local overlap matrix and $\mathbf{F}^s(E)$ represents the local Fock matrix including the interaction with the electric field E. The Fermi level $\varepsilon_F(E)$ can be determined by the constraint of the total number of electrons n_{e}:

$$n_e = \sum_s Tr[\mathbf{D}^s(E)\mathbf{S}^s]. \tag{12}$$

One can then obtain the density matrix of the entire system from Eqs. (8) and (9). The entire Fock matrix $\mathbf{F}(E)$ can be constructed in the usual manner:

$$F_{\mu\nu}(E) = H^{\mathrm{core}}_{\mu\nu} + E\cdot d_{\mu\nu} + \sum_s D^s_{\sigma\lambda}(E)[(\mu\nu|\lambda\sigma) - 1/2(\mu\sigma|\lambda\nu)], \tag{13}$$

with two electron integral notation of $(\mu\nu|\lambda\sigma) = \iint \mu^*(r_1)\nu(r_1)r_{12}^{-1}\lambda^*(r_2)\sigma(r_2)dr_1dr_2$, core Hamiltonian matrix $\mathbf{H}^{\mathrm{core}}$, and dipole moment matrix $\mathbf{d}$. As the standard SCF procedure, Fock matrix and density matrix constructions are iterated until convergence. Finally, the DC–HF energy $W^{\mathrm{DC}}_{\mathrm{HF}}$ is given as

$$W^{\mathrm{DC}}_{\mathrm{HF}}(E) = \frac{1}{2}\sum_s Tr[\mathbf{D}^s(E)\{\mathbf{H}^{\mathrm{core,s}} + E\cdot\mathbf{d}^s + \mathbf{F}^s(E)\}]. \tag{14}$$

In the DC–DFT calculation, the Fock matrix of Eq. (13) and the energy expression of Eq. (14) are substituted with the Kohn–Sham Hamiltonian and energy, respectively.

The DC-based correlation energy is obtained by means of the energy density analysis (EDA) [39], which adopts the energy partitioning analogous to Mulliken population analysis [40]. Hereafter, we omit the external field E since the effect of E appears indirectly in the correlation energy through the change in MOs. In the closed-shell case, the correlation energy is expressed in terms of active occupied orbitals $\{i, j\}$ and virtual orbitals $\{a, b\}$ as follows [41]:

$$\begin{aligned} W_{\mathrm{corr}} &= \sum_{ij}^{\mathrm{occ}}\sum_{ab}^{\mathrm{vir}} (ia|jb)[2\tilde{t}_{ij,ab} - \tilde{t}_{ij,ba}] \\ &= \sum_{ij}^{\mathrm{occ}}\sum_{ab}^{\mathrm{vir}} (ia|jb)[\tilde{S}_{ij,ab} + \tilde{T}_{ij,ab}]. \end{aligned} \tag{15}$$

Here, $\tilde{t}_{ij,ab}$ represents an effective two-electron excitation coefficient, and $\tilde{S}_{ij,ab} = \tilde{t}_{ij,ab}$ and $\tilde{T}_{ij,ab} = \tilde{t}_{ij,ab} - \tilde{t}_{ij,ba}$ are the singlet- and triplet-type redefined coefficients, respectively. In the DC calculation, the correlation energy corresponding to the subsystem s is represented on the analogy of EDA as follows:

$$\begin{aligned} W^s_{\mathrm{corr}} &= \sum_{ij}^{\mathrm{occ(s)}}\sum_{ab}^{\mathrm{vir(s)}}\sum_{\mu\in\boldsymbol{S}(s)} C^{s*}_{\mu i}(\mu a^s|j^s b^s)[2\tilde{t}^s_{ij,ab} - \tilde{t}^s_{ij,ba}] \\ &= \sum_{ij}^{\mathrm{occ(s)}}\sum_{ab}^{\mathrm{vir(s)}}\sum_{\mu\in\boldsymbol{S}(s)} C^{s*}_{\mu i}(\mu a^s|j^s b^s)[\tilde{S}^s_{ij,ab} + \tilde{T}^s_{ij,ba}], \end{aligned} \tag{16}$$

where occ(s) refers to local occupied orbitals in subsystem s, which have orbital energies lower than the Fermi level ε_{F}, and vir(s) to those having orbital energies higher than ε_{F}. Subsystem coefficients are evaluated in the subsystem s, namely in the MP2 case,

$$\tilde{t}^s_{ij,ab} = -\frac{(a^s i^s|b^s j^s)}{\varepsilon^s_a + \varepsilon^s_b - \varepsilon^s_i - \varepsilon^s_j}, \tag{17}$$

with $\tilde{S}^s_{ij,ab} = \tilde{t}^s_{ij,ab}$ and $\tilde{T}^s_{ij,ab} = \tilde{t}^s_{ij,ab} - \tilde{t}^s_{ij,ba}$.

In the following applications, we adopted the spin-component scaled MP2 (SCS–MP2) method, which was proposed by Grimme [42] as a facile procedure to improve the MP2 results. In the SCS–MP2 method, the singlet- and triplet-type contributions are individually scaled with two parameters w_{S} and w_{T}, giving the energy expression of

$$W^{s}_{\mathrm{corr}} = \sum_{ij}^{\mathrm{occ(s)}} \sum_{ab}^{\mathrm{vir(s)}} \sum_{\mu \in \boldsymbol{S}(s)} C^{s*}_{\mu i} (\mu a^{s} | j^{s} b^{s}) [w_{\mathrm{S}} \tilde{S}^{s}_{ij,ab} + w_{\mathrm{T}} \tilde{T}^{s}_{ij,ab}]. \tag{18}$$

Grimme [42] has proposed the optimized parameters as $w_{\mathrm{S}} = 6/5$ and $w_{\mathrm{T}} = 1/3$, which we adopted in the following SCS–MP2 calculations.

3 Numerical applications

We assessed the present DC–FF method in the (hyper)polarizability calculations of polyene chains and their derivatives with terminal donor or acceptor substituent, X–(CH=CH)$_n$–H (X=H, NH_2, and CN). Aoki et al. [29] applied the elongation FF method to the same systems and clarified that the substituent effect is greater in first hyperpolarizability β than those in polarizability α and second hyperpolarizability γ. We did not discuss the computational cost of the DC method in this paper because the costs for a FF calculation is completely proportional to those for energy calculations, which has been discussed in many previous papers [15, 18–22, 26, 27]. The z-axis was set to be parallel to the longitudinal axis of the molecule. The strength of the applied field, i.e., E_z in (5), (6), and (7), is set to be 0.0005 a.u. unless otherwise noted. All calculations presented in this section were performed with the 6-31G** basis set [43, 44]. The structures for X=H were fixed with uniform bond lengths and angles: 135.7, 146.2, and 109.6 pm for the C=C, C–C, and C–H lengths, respectively, and 120° for the ∠C–C–C and ∠H–C–C angles. The geometrical parameters regarding the substituents were determined by locally optimizing the geometry of X–(CH=CH)$_2$–H at the B3LYP [45, 46] level of theory with the 6-31G** basis set. In the DC calculation, a C_2H_2 (or C_2H_2X, for the edges) unit was adopted as a central region and several adjacent units were treated as the corresponding buffer region. The size of the buffer region is denoted by n_{b} which indicates that each left and right buffer region contains up to n_{b} units. The inverse temperature β_{temp} appearing in Eq. (9) was set to 200 a.u.

At first, we examined the buffer-size dependence of the accuracy of the linear polarizability calculated by the DC–HF method. Table 1 shows the polarizability α_{zz} and field-free total energy $W(0)$ of a polyene chain, H–(CH=CH)$_{24}$–H, calculated by the DC–HF method with $n_{\mathrm{b}} = 5$–11. The values obtained by the conventional HF method are also listed at the bottom. The percent error of the DC polarizability, $100(\alpha^{\mathrm{DC}} - \alpha^{\mathrm{conv}})/\alpha^{\mathrm{conv}}$, and the difference error of the DC energy, $W^{\mathrm{DC}}(0) - W^{\mathrm{conv}}(0)$, are shown in parentheses in Table 1. As previously reported [15, 26], the total energy error decreases to zero exponentially as the buffer size increases. Regarding the test system, the energy error achieves less than 1 mhartree, namely, chemical accuracy, for $n_{\mathrm{b}} \geq 6$. In a similar way, the polarizability error decreases exponentially with respect to the buffer size. This decay behavior of the errors can be interpreted by considering the real-space one-particle density matrix, $\rho(r, r') = \sum_{\lambda\sigma} D_{\lambda\sigma} \phi_{\lambda}(r) \phi_{\sigma}{}^{*}(r')$, falling off exponentially as $|r - r'| \to \infty$ in non-metallic cases, as discussed in the previous paper [16] in energy.

The absolute error of the polarizability obtained by the present DC–FF method is compared with that by the DC-based TDCP HF (DC–TDCPHF) method [24], in which the polarizability is evaluated with the z-direction induced density matrix $\mathbf{D}^{z}$ and dipole moment matrix, $d^{z}_{\mu\nu} = -\langle \mu | z | \nu \rangle$, as

$$\alpha_{zz} = \mathrm{Tr}[\mathbf{D}^{z}\mathbf{d}^{z}], \tag{19}$$

in Fig. 1. Although both errors decrease exponentially with respect to the buffer size, the DC–TDCPHF method tends to offer fast convergence for the buffer size. However, the difference between these two methods diminishes as the buffer size increases. This tendency can be explained by the denominator of Eq. (5), being $E_z^{-2} \sim 10^6$ a.u. Although the error of the numerator of Eq. (5), which is quadratic with respect to the density matrix error, is enhanced in the DC–FF method, the error of Eq. (19) is only linear to that of the induced density matrix by the DC–TDCPHF method.

Next, we discuss the system-size dependence of the calculated polarizability α_{zz} by changing the length of the polyene chain, H–(CH=CH)$_n$–H for $n = 24$–84, which is summarized in Fig. 2. The data obtained by the DC–HF method with $n_{\mathrm{b}} = 9$ and 11 are plotted together with the conventional HF data. In the calculations for $n \geq 72$, we used $E_z = 0.0001$ a.u. as the strength of the applied field instead of $E_z = 0.0005$ a.u., because the SCF iteration failed to converge when adopting a stronger field strength. As the chain length increases, the calculated polarizability increases quasi-linearly. It was confirmed that for the DC result with $n_{\mathrm{b}} = 9$ the discrepancy of the polarizability from the conventional result increases as the system size increases. For $n = 84$, the percent error becomes 17.4% as compared to 0.4% for $n = 24$. This discrepancy significantly diminishes by adopting larger buffer size, namely for $n_{\mathrm{b}} = 11$, the percent error for $n = 84$ is 2.5%.

We also tested the wavefunction-based correlation theories. Figure 3 shows the polarizability α_{zz} obtained by the DC and conventional MP2, SCS-MP2, and coupled-cluster with single and double excitations (CCSD) calculations of the polyene chains, H–(CH=CH)$_n$–H for $n = 8$–48. The conventional HF and DFT results with BLYP [47, 48] and long-range corrected BLYP (LC–BLYP) [49] functionals

Table 1 The polarizability α_{zz} and field-free total energy $W(0)$ of a polyene chain, H–(CH=CH)$_{24}$–H, calculated at the DC–HF/6–31G** level with $n_b = 5$–11

n_b	α_{zz} [a.u.]	(% Error)	$W(0)$ [hartree]	(Diff.) [mhartree]
5	4,332.4	(+27.8)	−1,846.489887	(+1.020)
6	3,687.5	(+8.8)	−1,846.490389	(+0.518)
7	3,484.9	(+2.8)	−1,846.490732	(+0.175)
8	3,419.9	(+0.9)	−1,846.490841	(+0.066)
9	3,398.9	(+0.3)	−1,846.490884	(+0.023)
10	3,392.2	(+0.1)	−1,846.490899	(+0.008)
11	3,390.1	(+0.0)	−1,846.490904	(+0.003)
Conv.	3,389.2		−1,846.490907	

The values obtained by the conventional HF method are also listed at the *bottom*. The percent error of the polarizability and the difference error of the energy from the conventional results are shown in *parentheses*

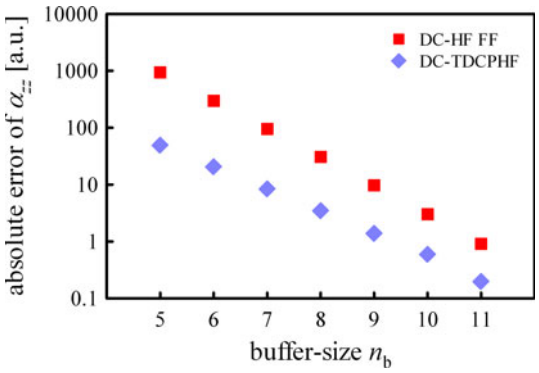

Fig. 1 The buffer-size dependence of the absolute error of the polarizability α_{zz} of a polyene chain, H–(CH=CH)$_{24}$–H, obtained by the DC–TDCPHF and the present DC–HF FF methods with 6–31G** basis set

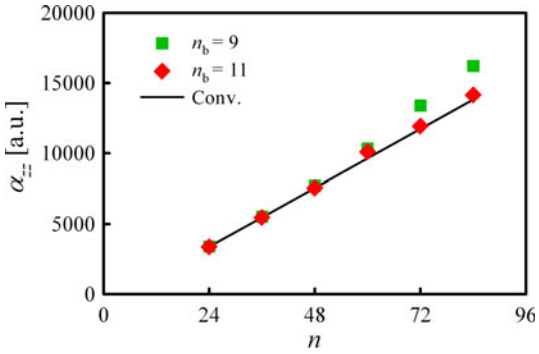

Fig. 2 The system-size dependence of the polarizability α_{zz} of polyene chains, H–(CH=CH)$_n$–H ($n = 24$–84), calculated at the DC ($n_b = 9$ or 11) and conventional HF methods with 6–31G** basis set

are shown together. Here, we obtained the polarizability values with energies at three electric fields as

$$\alpha_{zz} = \frac{W(+E_z) - 2W(E_z) + W(-E_z)}{E_z^2}, \qquad (20)$$

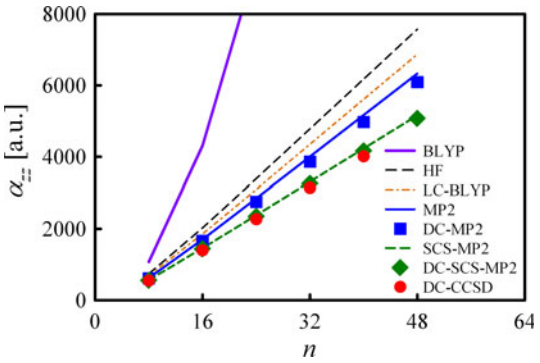

Fig. 3 The system-size dependence of the polarizability α_{zz} of polyene chains, H–(CH=CH)$_n$–H ($n = 8$–48), calculated at the DC with $n_b = 3$ (*symbols*) and conventional (*lines*) MP2, SCS–MP2, and CCSD (DC only) methods with 6–31G** basis set. The conventional HF and DFT results are shown together

with $E_z = 0.001$ a.u., instead of Eq. (5) using five electric fields. For DC calculations, we used the dual-buffer scheme [21] where the HF calculation is performed in the conventional manner and the correlation energy is obtained by the DC method. The buffer size for the DC correlation calculation was set to $n_b = 3$. The CCSD results were only available with the DC method due to its tremendous computational costs. In the MP2 and SCS–MP2 calculations, the polarizability error introduced by the DC method is sufficiently small: the mean absolute percent errors of the DC–MP2 and DC–SCS–MP2 polarizabilities from the conventional method are 3.0 and 1.2%, respectively. Since the CCSD correlation energy error introduced by the DC method is comparable to the MP2 one [19], the DC–CCSD result is considered to be most accurate in Fig. 3. The DFT results adopting the standard functional (e.g., BLYP) overestimate the polarizabilitiy of large π-conjugated systems, as is reported previously [49–51]. Although the LC scheme clearly improves the calculated polarizability values for these systems, there is still significant difference in α_{zz} value between LC–BLYP and CCSD results. Both DC

Table 2 The field-strength (E_z) dependence of α_{zz}, β_{zzz}, and γ_{zzzz} of a polyene chain with terminal acceptor substituent, CN–$(CH{=}CH)_{16}$–H, at the DC–SCS-MP2/6–31G** level

E_z [a.u.]	α_{zz} [10^3 a.u.]				β_{zzz} [10^4 a.u.]				γ_{zzzz} [10^7 a.u.]			
	Conv.	(% Dev.)	DC	(% Dev.)	Conv.	(% Dev.)	DC	(% Dev.)	Conv.	(% Dev.)	DC	(% Dev.)
0.000125	1.553	(−0.0)	1.563	(+0.8)	3.581	(+4.2)	10.77	(+220)	12.49	(+82.1)	−228.4	(−3,530)
0.00025	1.554	(+0.0)	1.550	(+0.0)	3.401	(−1.0)	3.324	(−1.0)	6.643	(−3.2)	5.932	(−10.8)
0.0005	1.554		1.550		3.437		3.357		6.861		6.651	
0.001	1.553	(−0.0)	1.550	(−0.0)	3.626	(+5.5)	3.531	(+5.2)	7.146	(+4.2)	6.946	(+4.4)
0.002	1.549	(−0.3)	1.546	(−0.3)	4.701	(+36.8)	4.479	(+33.4)	8.582	(+25.1)	8.227	(+23.7)
0.004	−0.294	(−119)	0.582	(−62.5)	−86.39	(−2,610)	41.62	(+1,140)	146.8	(+2,040)	80.54	(+1,110)

The percent deviations from the result with $E_z = 0.0005$ a.u. are shown in *parentheses*

Table 3 The buffer-size dependence of α_{zz}, β_{zzz}, γ_{zzzz}, and $W(0)$ of a polyene chain with terminal acceptor substituent, CN–$(CH{=}CH)_{24}$–H, at the DC–SCS-MP2/6–31G** level

n_b	α_{zz} [10^3 a.u.]	(% Error)	β_{zzz} [10^4 a.u.]	(% Error)	γ_{zzzz} [10^8 a.u.]	(% Error)	$W(0)$ [hartree]	(Diff.) [mhartree]
3	2.438	(−1.1)	3.321	(−11.0)	1.233	(−11.3)	−1,944.767028	(+1.948)
4	2.444	(−0.9)	3.537	(−6.7)	1.313	(−7.2)	−1,944.768204	(+0.771)
5	2.455	(−0.5)	3.678	(−3.9)	1.367	(−4.3)	−1,944.768738	(+0.237)
6	2.462	(−0.3)	3.763	(−2.2)	1.401	(−2.5)	−1,944.768894	(+0.081)
7	2.467	(−0.1)	3.813	(−1.3)	1.422	(−1.4)	−1,944.768948	(+0.028)
8	2.469	(−0.1)	3.841	(−0.7)	1.434	(−0.8)	−1,944.768966	(+0.009)
Conv.	2.470		3.876		1.449		−1,944.768975	

The percent errors of the polarizabilities and the difference errors of the energy from the conventional values are shown in *parentheses*

and conventional (SCS–)MP2 methods give better results than LC–BLYP. In particular, the polarizability obtained by SCS–MP2 agrees fairly well with that by DC–CCSD in this system, although the parameters involved in the SCS–MP2 method were optimized for reproducing the reaction energies. The DC method not only reduced the computational cost of the correlation calculation, but also revealed that the SCS–MP2 scheme works well even for the polarizability calculation.

From here, we discuss the calculated hyperpolarizabilities in addition to the linear polarizability. First, we assessed the field-strength (E_z) dependence of the accuracy of the (hyper)polarizabilities. Table 2 shows the polarizability α_{zz}, first hyperpolarizability β_{zzz}, and second hyperpolarizability γ_{zzzz} of a polyene chain with terminal acceptor substituent, CN–$(CH{=}CH)_{16}$–H, obtained using Eqs. (5), (6), and (7) adopting DC–SCS–MP2 energies with the fixed correlation buffer size of $n_b = 6$. Only the correlation energies were obtained in the DC manner. The values obtained by the conventional SCS–MP2 method are listed as well. The percent deviations from the result with $E_z = 0.0005$ a.u., which we have adopted, are shown in parentheses. The deviation of α_{zz} is within ±0.8% for $E_z \leq 0.002$ a.u. When adopting the stronger electric field strength of $E_z = 0.004$ a.u., the calculated polarizability gives an unphysical result, i.e., a negative value for the conventional method, because the perturbative expansion of Eq. (1) breaks down for the stronger electric field strength. On the other hand, when adopting the weaker electric field strength of $E_z = 0.000125$ a.u., the calculated β_{zzz} and γ_{zzzz} values significantly deviate from the values for 0.00025 a.u. $\leq E_z \leq$ 0.002 a.u. due to the numerical differentiation of Eqs. (5), (6), and (7) using energies with limited accuracy (the SCF convergence criteria was set to 2×10^{-7} in the largest density matrix change). For 0.00025 a.u. $\leq E_z \leq$ 0.001 a.u., the deviations of α_{zz}, β_{zzz}, and γ_{zzzz} are rather small, being ±0.0, ±5.5, and ±10.8%, respectively. The following calculations, therefore, adopted $E_z = 0.0005$ a.u.

Next, we assessed the buffer-size dependence of the (hyper)polarizabilitiies, α_{zz}, β_{zzz}, and γ_{zzzz}, and field-free total energy $W(0)$ of a CN–$(CH{=}CH)_{24}$–H system calculated by the DC–SCS–MP2 method with $n_b = 3$–8 correlation buffer, which is summarized in Table 3. The values obtained by the conventional SCS–MP2 method are also listed at the bottom. All errors given in Table 3 decrease to 0 as the buffer size increases. We confirmed that the DC–SCS–MP2 method can evaluate the polarizability accurately with smaller buffer size than DC–HF does (compare with Table 1). Although larger buffer size is required to accurately evaluate the first and second hyperpolarizabilities, it was confirmed that the use of $n_b = 6$ achieves 2.5% or less errors in hyperpolarizability values.

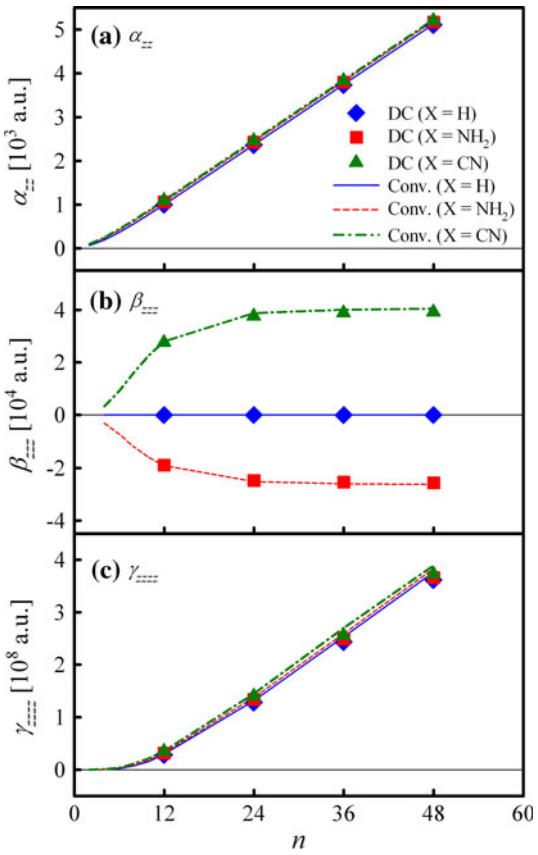

Fig. 4 The system-size dependence of the (hyper)polarizabilities [(**a**) α_{zz}, (**b**) β_{zzz}, (**c**) γ_{zzzz}] of the polyene derivatives, X–(CH=CH)$_n$–H (X=H, NH_2, and CN, $n = 12$–48), obtained by the DC and conventional SCS–MP2 method. The correlation buffer size was fixed at $n_b = 6$ in DC calculations

Finally, we compare the molecular size dependence of the (hyper)polarizabilities of the polyene and its derivatives, X–(CH=CH)$_n$–H (X=H, NH_2, CN). Figure 4 shows (a) the polarizability α_{zz}, (b) first hyperpolarizability β_{zzz}, and (c) second hyperpolarizability γ_{zzzz} obtained by the DC and conventional SCS–MP2 calculations of these molecules with $n = 12$–24. The data for $n = 2$–10 are also plotted in the conventional SCS–MP2 results. The correlation buffer size was fixed at $n_b = 6$. From the SCS–MP2 result in Fig. 4a, c, the increments in the polarizability α_{zz} and second hyperpolarizability γ_{zzzz} due to enlargement of the molecular size do not depend on substituent X. Although the second hyperpolarizability shows non-linear dependence on the system size for smaller molecules, it changes to the linear dependence for $n \geq 12$. The first hyperpolarizabilities β_{zzz} of X=H in Fig. 4b are zero because of the molecular symmetry. The β_{zzz} values are nearly constant against the change of the chain length but highly dependent upon substituent X. The DC–SCS–MP2 method finely reproduces the conventional results. The mean absolute percent errors of α_{zz}, β_{zzz}, and γ_{zzzz} from the conventional results become 0.3, 2.3, and 3.5%, respectively. Although these behaviors of α_{zz}, β_{zzz}, and γ_{zzzz} are qualitatively consistent with the previous reports [29, 52], the absolute values are considerably different: e.g., α_{zz} values of X–(CH=CH)$_{24}$–H are around 3,800, 3,200, and 1,100 a.u. by the PM3 [29], HF/6-31G [52], and present MP2/6-31G** calculations. It was confirmed that the incorporation of the electron correlation as well as the polarization basis functions significantly affects the absolute values.

4 Concluding remarks

In the present study, we have implemented for the first time the FF evaluation of molecular static (hyper)polarizabilities in the framework of the linear-scaling DC treatment. The introduction of the external electric field to the DC method is straightforwardly accomplished by adding the interaction term to the Fock matrix. The effectiveness of the present DC–FF method was demonstrated in the calculations of π-conjugated systems. It was confirmed that the error of the polarizability introduced by the DC treatment decreases exponentially to zero with respect to the buffer size, as well as the total energy. This behavior assures that one will obtain sufficiently accurate results by adopting an

Table 4 The basis-set dependence of α_{zz}, β_{zzz}, and γ_{zzzz} of a polyene chain with terminal acceptor substituent, CN–(CH=CH)$_{16}$–H, at the DC–SCS-MP2 level

Basis set	α_{zz} [10^3 a.u.]			β_{zzz} [10^4 a.u.]			γ_{zzzz} [10^7 a.u.]		
	Conv. [%]	DC	(% Error)	Conv. [%]	DC	(% Error)	Conv. [%]	DC	(% Error)
6–31G**	1.554 [90.4]	1.550	(−0.2)	3.437 [90.7]	3.357	(−2.3)	6.861 [76.2]	6.651	(−3.1)
6–311G**	1.660 [96.6]	1.655	(−0.3)	3.623 [95.6]	3.526	(−2.7)	7.843 [87.1]	7.626	(−2.8)
6–31++G**	1.675 [97.5]	1.663	(−0.7)	3.790 [100.0]	4.094	(+8.0)	7.928 [88.1]	7.718	(−2.6)
6–311++G**	1.719	1.715	(−0.2)	3.790	3.472	(−8.4)	9.000	8.258	(−8.2)
MA%E			(0.4)			(5.3)			(4.2)

For conventional calculations, the ratios to the 6–311++G** results are given in *square brackets*. The percent errors of the DC results from the conventional values are shown in *round parentheses*, of which MA%Es are given on the *bottom*

appropriate buffer size, although the polarizability error of the DC–HF FF method is larger than that of the DC–TDCPHF method previously reported [24] when the same buffer size is adopted. In addition, the DC–FF approach is applicable to the electron correlation theories where the DC method performs quite efficiently: this combination enables the CCSD polarizability evaluation of large systems. In the present calculations, SCS–MP2 polarizability agrees well with the CCSD one. We also showed that the DC–FF method reproduces well the first and second hyperpolarizabilities for homogenous and heterogeneous systems. In conclusion, the present DC–FF method is regarded as a powerful tool for the computer-aided electro-optical material development.

In this paper, we only focused on the evaluation of static optical properties. However, for enabling the theoretical design of actual devices, the evaluation of dynamic optical properties will be desired. For obtaining dynamic properties, we have proposed a scheme based on the TDCP equations [24] within the HF framework. Although its extension to DFT is straightforward by employing the induced DFT Hamiltonian matrix instead of the Fock matrix, it is difficult to extend it to ab initio correlation level of theories, requiring the expensive procedure for obtaining analytic derivatives. Rice and Handy [53], for instance, proposed the pseudo-energy derivatives (PED) method as a scheme to obtain dynamic properties. The combination of PED with the DC method is a possible candidate for the linear-scaling evaluation of the ab initio dynamic optical properties. Furthermore, we are now investigating a method to obtain dynamic hyperpolarizabilities within the HF/DFT level of theory by extending the DC–TDCPHF method, which will appear elsewhere.

Acknowledgments Some of the present calculations were performed at the Research Center for Computational Science (RCCS), Okazaki Research Facilities, National Institutes of Natural Sciences (NINS). This study was supported in part by Grants-in-Aid for Challenging Exploratory Research "KAKENHI 22655008" and for Young Scientists (B) "KAKENHI 22750016" from the Ministry of Education, Culture, Sports, Science and Technology (MEXT), Japan; by the Nanoscience Program in the Next Generation Super Computing Project of the MEXT; by the Global Center Of Excellence (COE) "Practical Chemical Wisdom" from the MEXT; and by a project research grant for "Practical in-silico chemistry for material design" from the Research Institute for Science and Engineering (RISE), Waseda University.

Appendix

The basis-set dependence of the present method were assessed in calculations of the CN–$(CH{=}CH)_{16}$–H system. Table 4 shows the static (hyper)polarizabilities evaluated by the DC (with fixed buffer size of $n_b = 6$) and conventional SCS-MP2 method with 6–311G** [54], 6–31++G** [43, 44, 55], and 6–311++G** [54, 55] basis sets in addition to the 6–31G** set. For conventional calculations, the ratios to the 6–311++G** results are given in square brackets. The (hyper)polarizability values systematically converge by improving the basis set, although α_{zz} and β_{zzz} values are less dependent on the adopted basis set than γ_{zzzz} value: the 6-31G** results reproduce 90.4, 90.7, and 76.2% of the 6–311++G** values for α_{zz}, β_{zzz}, and γ_{zzzz}, respectively. One should pay close attention to the adopting basis sets for the quantitative discussion about the γ_{zzzz} value. Looking at the DC results, of which the percent errors from the conventional values are shown in round parentheses, the errors introduced by the DC method are smaller than those by the adopted basis set: the mean absolute percent errors (MA%Es) are 0.4, 5.3, and 4.2% for α_{zz}, β_{zzz}, and γ_{zzzz}, respectively. It was also confirmed that larger errors can be found for the hyperpolarizability values when adopting a basis set with diffuse functions.

References

1. Yesodhaa SK, Sadashiva Pillaia CK, Tsutsumi N (2004) Prog Polym Sci 29:45
2. Huanga JP, Yu KW (2006) Phys Rep 431:87
3. Choa MJ, Choia DH, Sullivanb PA, Akelaitis AJP, Daltonb LR (2008) Prog Polym Sci 33:1013
4. Khoo IC (2009) Phys Rep 471:221
5. Imamura A, Aoki Y, Maekawa K (1991) J Chem Phys 95:5419
6. Aoki Y, Suhai S, Imamura A (1994) Int J Quantum Chem 52:267
7. Makowski M, Korchowiec J, Gu FL, Aoki Y (2010) J Comput Chem 31:1733
8. Korchowiec J, Gu FL, Aoki Y (2005) Int J Quantum Chem 105:875
9. Gu FL, Aoki Y, Korchowiec J, Imamura A, Kirtman B (2004) J Chem Phys 121:10385
10. Korchowiec J, Gu FL, Imamura A, Kirtman B, Aoki Y (2005) Int J Quantum Chem 102:785
11. Korchowiec J, Lewandowski J, Makowski M, Gu FL, Aoki Y (2009) J Comput Chem 30:2515
12. Aoki Y, Gu FL (2009) In: Proceedings of the international conference of computational methods in sciences and engineering (ICCMSE 2009) AIP conference proceeding
13. Yang W (1991) Phys Rev Lett 66:1438
14. Yang W, Lee TS (1995) J Chem Phys 103:5674
15. Akama T, Kobayashi M, Nakai H (2007) J Comput Chem 28:2003
16. Akama T, Fujii A, Kobayashi M, Nakai H (2007) Mol Phys 105:2799
17. Kobayashi M, Akama T, Nakai H (2006) J Chem Phys 125:204106
18. Kobayashi M, Imamura Y, Nakai H (2007) J Chem Phys 127:074103
19. Kobayashi M, Nakai H (2008) J Chem Phys 129:044103
20. Kobayashi M, Nakai H (2009) J Chem Phys 131:114108
21. Kobayashi M, Nakai H (2009) Int J Quantum Chem 109:2227
22. Kobayashi M, Yoshikawa T, Nakai H (2010) Chem Phys Lett 500:172

23. Kobayashi M, Kunisada T, Akama T, Sakura D, Nakai H (2011) J Chem Phys 134:034105
24. Touma T, Kobayashi M, Nakai H (2010) Chem Phys Lett 485:247
25. Schmidt MW, Baldridge KK, Boatz JA, Elbert ST, Gordon MS, Jensen JH, Koseki S, Matsunaga N, Nguyen KA, Su S, Windus TL, Dupuis M, Montgomery JA Jr (1993) J Comput Chem 14:1347
26. Kobayashi M, Nakai H (2011) Divide-and-conquer approaches to quantum chemistry: Theory and implementation. In: Papadopoulos MG, Zalesny R, Mezey PG, Leszczynski J (eds) Linear-scaling techniques in computational chemistry and physics. Springer, Berlin, pp 97–127
27. Kobayashi M, Akama T, Nakai H (2009) J Comput Chem Jpn 8:1
28. Gu FL, Aoki Y, Imamura A, Bishop DM, Kirtman B (2003) Mol Phys 101:1487
29. Ohnishi S, Gu FL, Naka K, Imamura A, Kirtman B, Aoki Y (2004) J Phys Chem A 108:8478
30. Ohnishi S, Orimoto Y, Gu FL, Aoki Y (2007) J Chem Phys 127:084702
31. Chen W, Yu G, Gu FL, Aoki Y (2009) Chem Phys Lett 474:175
32. Yu GT, Chen W, Gu FL, Aoki Y (2010) J Comput Chem 31:863
33. Pomogaeva A, Gu FL, Imamura A, Aoki Y (2010) Theor Chem Acc 125:453
34. Yan LK, Pomogaeva A, Gu FL, Aoki Y (2010) Theor Chem Acc 125:511
35. Fedorov DG, Kitaura K (2007) J Phys Chem A 111:6904
36. Fedorov DG, Kitaura K (eds) (2009) The fragment molecular orbital method: practical applications to large molecular systems. CRC Press, Boca Raton
37. Mochizuki Y, Ishikawa T, Tanaka K, Tokiwa H, Nakano T, Tanaka S (2006) Chem Phys Lett 418:418
38. Ishikawa T, Mochizuki Y, Imamura K, Nakano T, Mori H, Tokiwa H, Tanaka K, Miyoshi E, Tanaka S (2006) Chem Phys Lett 430:361
39. Nakai H (2002) Chem Phys Lett 363:73
40. Mulliken RS (1955) J Chem Phys 23:1833
41. Nesbet RK (1969) Adv Chem Phys 14:1
42. Grimme S (2003) J Chem Phys 118:9095
43. Hehre WJ, Ditchfield R, Pople JA (1972) J Chem Phys 56:2257
44. Hariharan PC, Pople JA (1973) Theor Chim Acta 28:213
45. Becke AD (1993) J Chem Phys 98:5648
46. Stephens PJ, Devlin FJ, Chabalowski CF, Frisch MJ (1994) J Phys Chem 98:11623
47. Becke AD (1988) Phys Rev A 38:3098
48. Lee C, Yang W, Parr RG (1988) Phys Rev B 37:785
49. Iikura H, Tsuneda T, Yanai T, Hirao K (2001) J Chem Phys 115:3540
50. Mosley DH, Champagne B, André JM (1995) Int J Quantum Chem 29:117
51. Champagne B, Perpète EA, van Gisbergen SJA, Baerends E-J, Snijders JG, Soubra-Ghaoui C, Robins KA, Kirtman B (1998) J Chem Phys 109:10489
52. Kirtman B, Toto JL, Robins KA, Hasan M (1995) J Chem Phys 102:5350
53. Rice JE, Handy NC (1991) J Chem Phys 94:4959
54. Krishnan R, Binkley JS, Seeger R, Pople JA (1980) J Chem Phys 72:650
55. Clark T, Chandrasekhar J, Spitznagel GW, Schleyer PvR (1983) J Comput Chem 4:294